Supplemental Materials

Molecular Biology of the Cell

Lovelace et al.

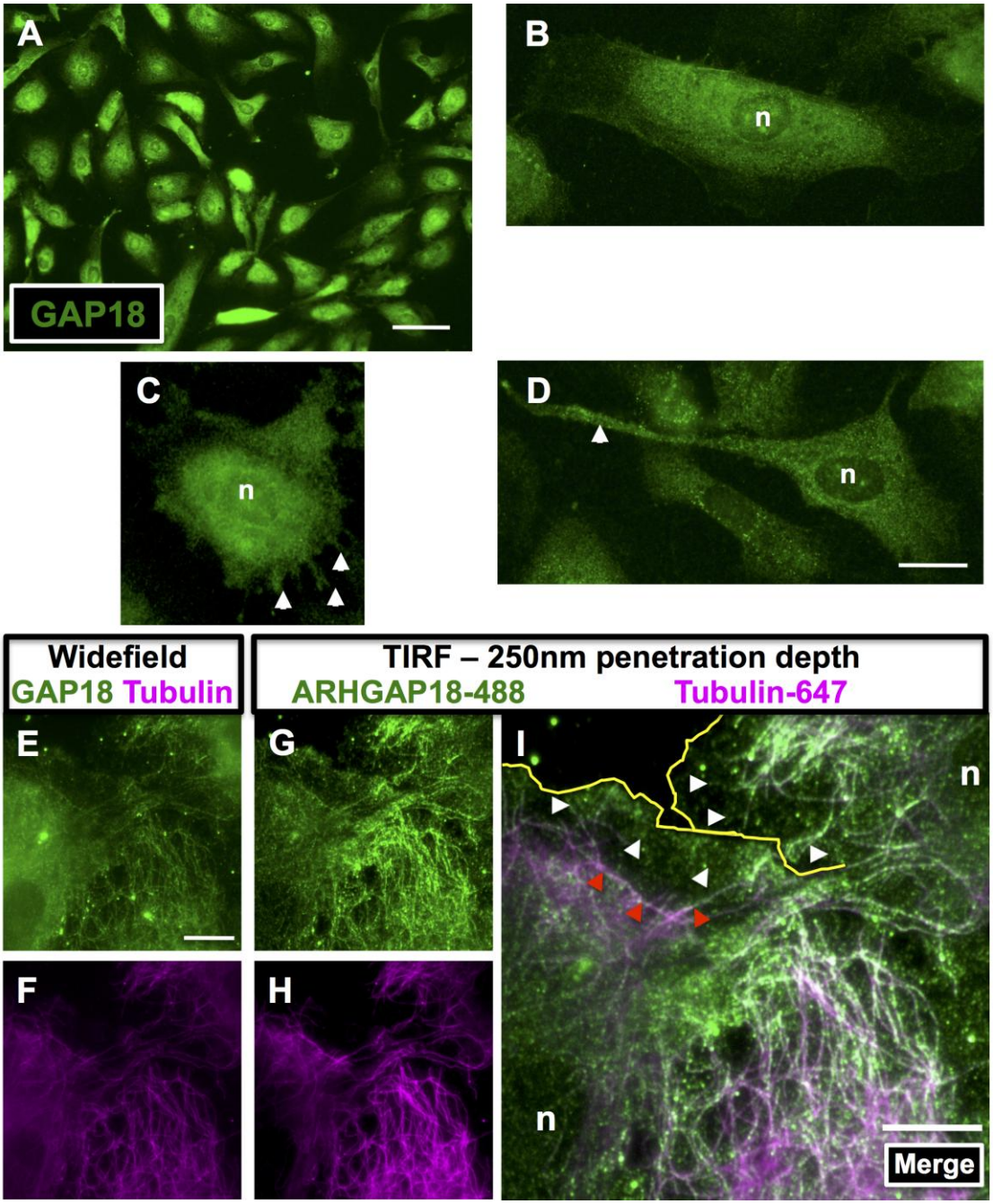

Fig.S1 (A-D) ARHGAP18 expression in EC's by widefield and TIRF microscopy Widefield imaging of ARHGAP18 staining shows broad expression in non-confluent ECs (**A**; 20x magnification). **(B-D)** High magnification (63x) images of ARHGAP18 staining in ECs with different morphologies. All four cells showed intense perinuclear immunoreactivity (indicated by n). **(B)** Bipolar flattened EC. **(C)** EC showing ARHGAP18 localised to thin processes (white arrowheads) and the cell periphery (yellow arrowhead). **(D)** Unipolar EC with ARHGAP18 immunoreactivity along an extended process (white arrow). Scale bar in **A** = 100µm, **D** = 20µm.

(E-I) TIRF imaging of ARHGAP18 and tubulin localisation in the fringe of 3 intersecting cells Compared to widefield imaging (**E**), TIRF imaging (**G**) greatly reduces the amount of perinuclear ARHGAP18 staining, and microtubules are also localised in the evanescent field **(**magenta; **F**, **H)**. **(I)** Merge of **(G** & **H)**. Note that the ARHGAP18 immunopositivity extends much further into the cell periphery (examples of immunopositivity shown by white arrowheads) than the extent of the

outermost microtubule filaments (example indicated by red arrowheads). The yellow line indicates the boundary (partially drawn) between the cells at the top right and bottom left, and is shown to highlight this staining pattern. n = nuclei. Scale bar in **E**, **I**= 10μm.

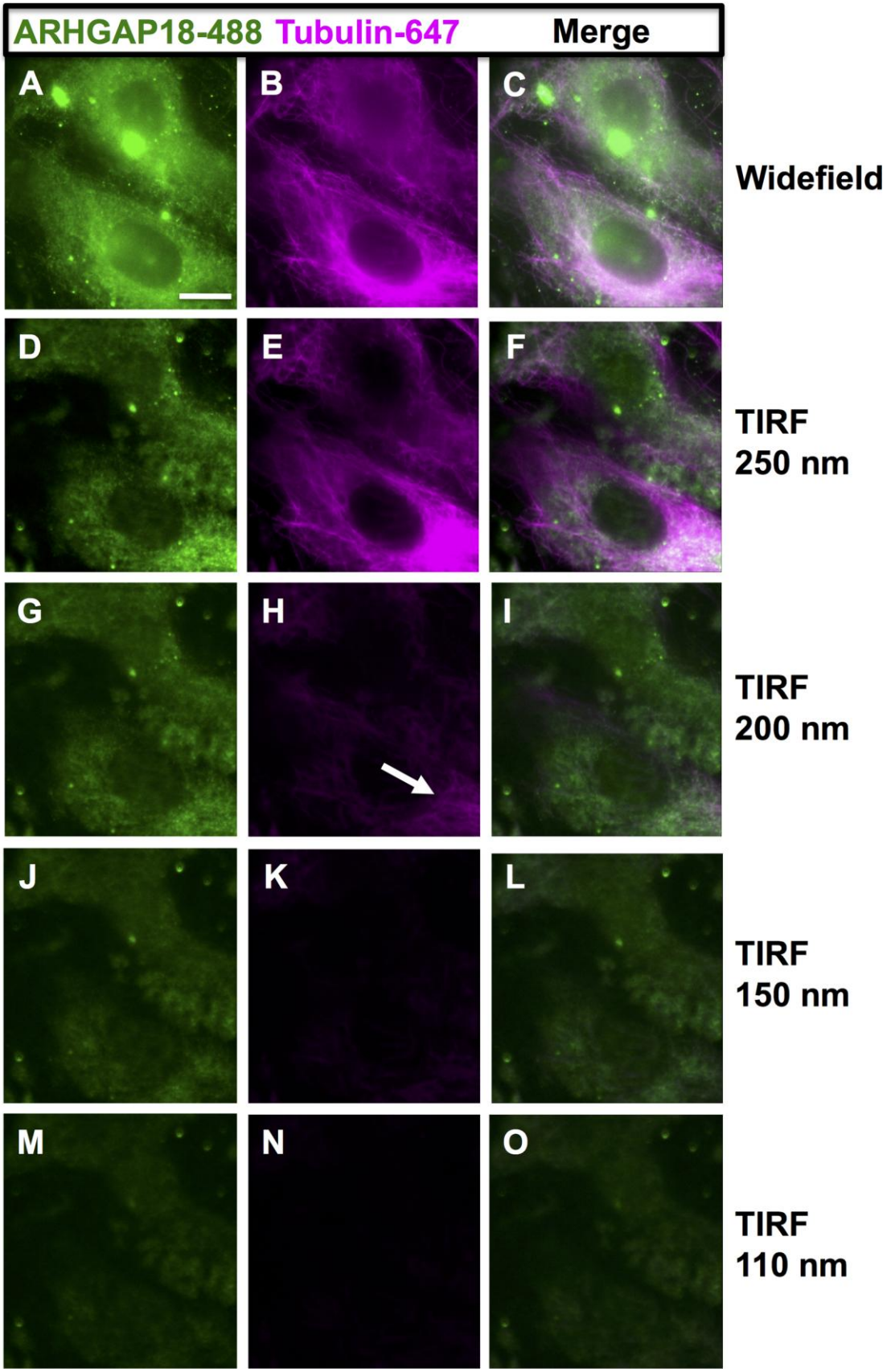

Fig.S2. ARHGAP18 and microtubules are localised close to the plasma membrane in ECs

TIRF penetration depths are indicated on the right hand side of the figure, and all image capture parameters (e.g. laser power and exposure) were kept identical between different depths and the images captured sequentially. Typical perinuclear ARHGAP18 expression **(A)** and microtubules **(B)** in two adjacent HUVECs imaged in widefield mode. **(C)** Merge of **(A)** and **(B)**. At 250nm penetration depth, some perinuclear ARHGAP18 immunoreactivity is lost **(D)**, while most microtubules still remain visible **(E, F)**. At 200nm penetration depth, there is very little alteration to ARHGAP18 staining **(G, I)**, while only faint perinuclear microtubule staining is present (**H**, white arrow). At 150nm and 110nm penetration depths (respectively), there is a progressive decrease in the intensity of ARHGAP18 staining **(J, L, M, O)**, while microtubule staining is completely absent **(K, N)**. This suggests that a proportion of the ARHGAP18 distribution is discrete from any localisation to microtubules i.e. is cytosolic.The decreased fluorescence seen at each penetration depth was not the result of photobleaching, as widefield images were also acquired at each depth, which did not show any noticeable decrease in staining intensity. Scale bar in **A** = 10μm.

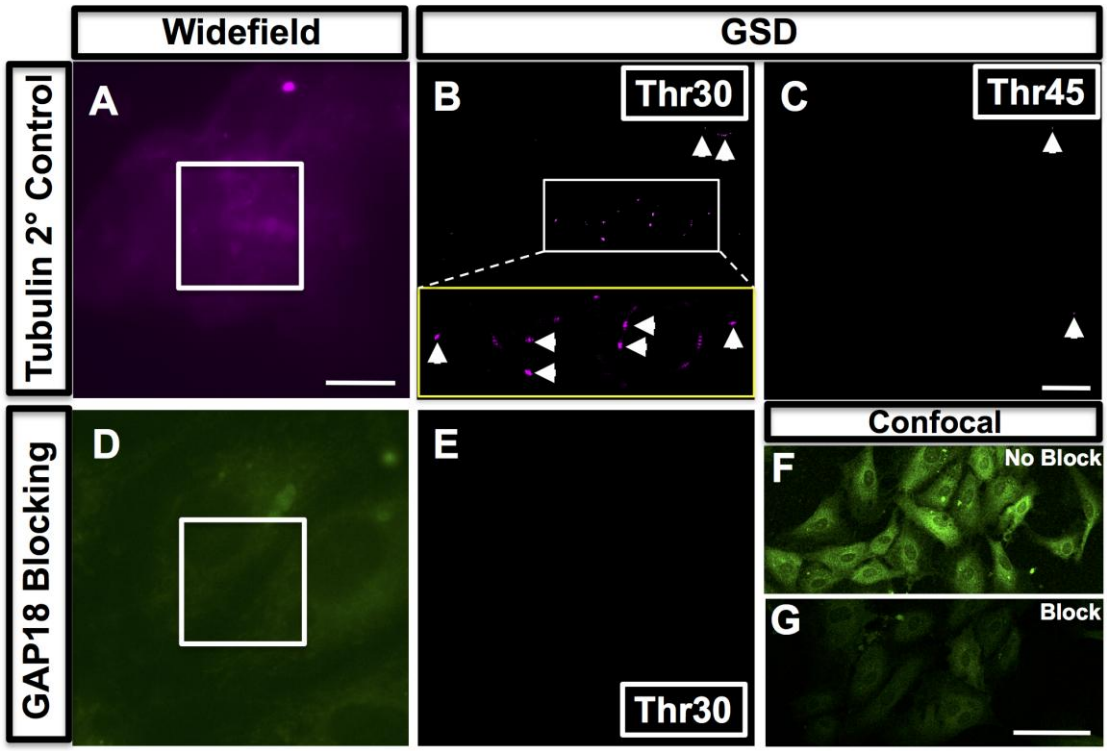

Fig.S3. Antibody controls for GSD microscopy(A-C) Secondary antibody only control shows the lack of non-specific staining on GSD with appropriate thresholding. **(A)**Widefield image (50 x 50μm) taken of typical field of view of a single HUVEC that has been stained with an anti-mouse Alexa 647 secondary antibody only, but with otherwise an identical procedure as that for staining with α-tubulin. Non-distinct fluorescence emission is observed. White boxes in (**A**) and (**D**) indicate areas that are imaged in GSD mode in **B**, **C**, **E**. **(B)** GSD image of the white box in (**A**), (17.2x17.2μm). A photon threshold of 30 was used, and identified some small isolated pixels that are likely background noise (white arrowsheads and white box, shown zoomed in yellow box). At least 18,000 frames were collected. **(C)**

Reconstruction of the same image in LAS AF software with a photon threshold of 45 (used for imaging tubulin in other GSD stainings) almost completely eliminated the noise (arrowheads). (**D**) Mixing of the 2A3-Alexa488 ARHGAP18 direct conjugate antibody with a five-fold excess of ARHGAP18 blocking peptide for 2 hours prior to overnight incubation with fixed and permeabilised cultured ECs shows lack of immunopositivity. (**E**) In GSD imaging mode of the same field, no events were detected with a photon threshold of 30 (used for imaging ARHGAP18 in other GSD stainings). At least 15,000 frames were collected. Confocal imaging (**F-G**) demonstrated a substantial reduction in staining intensity with blocking peptide. Scale bar in **A**= 10µm, **C**= 2.5µm,**G**= 50µm.

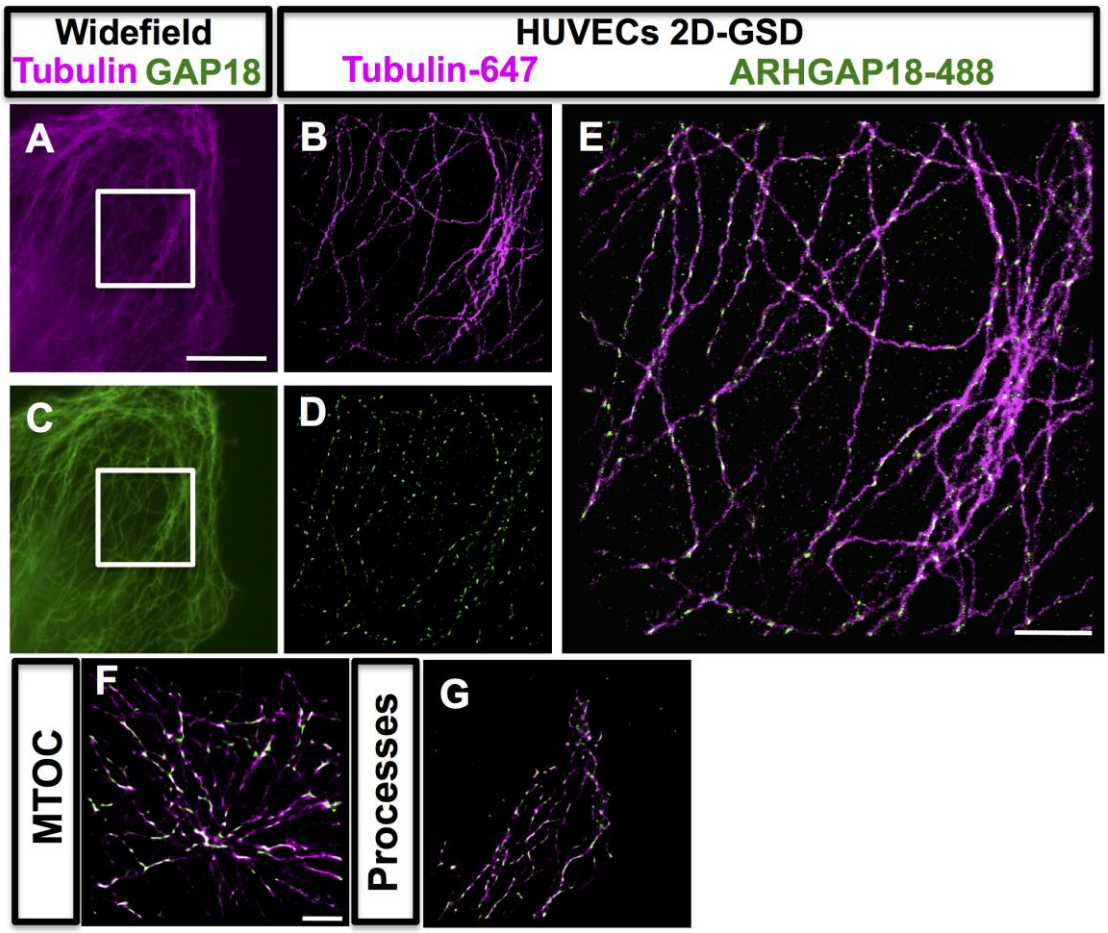

Fig.S4. ARHGAP18 is present on complex networks of MTs found in the leading edge of an EC, and in different regions of ECs. Widefield**(A, C)** and images resolved in GSD mode **(B, D,** merged in **E)** showed ARHGAP18 regularly spaced along the microtubule filaments. Imaging in different regions of ECs also showed that ARHGAP18 is localised to microtubule filaments in these regions – the microtubule organising centre (MTOC; **F**) and extended processes (**G**). Scale bar in **A** = 10µm; **E, F** = 2.5µm.

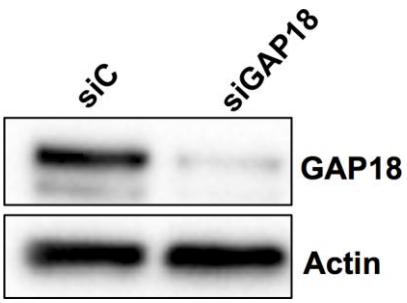

Fig.S5 Representative western blot for levels of ARHGAP18 in EC following 48 hours culture after transfection of siRNAs for control (siC) or ARHGAP18 (siGAP18).

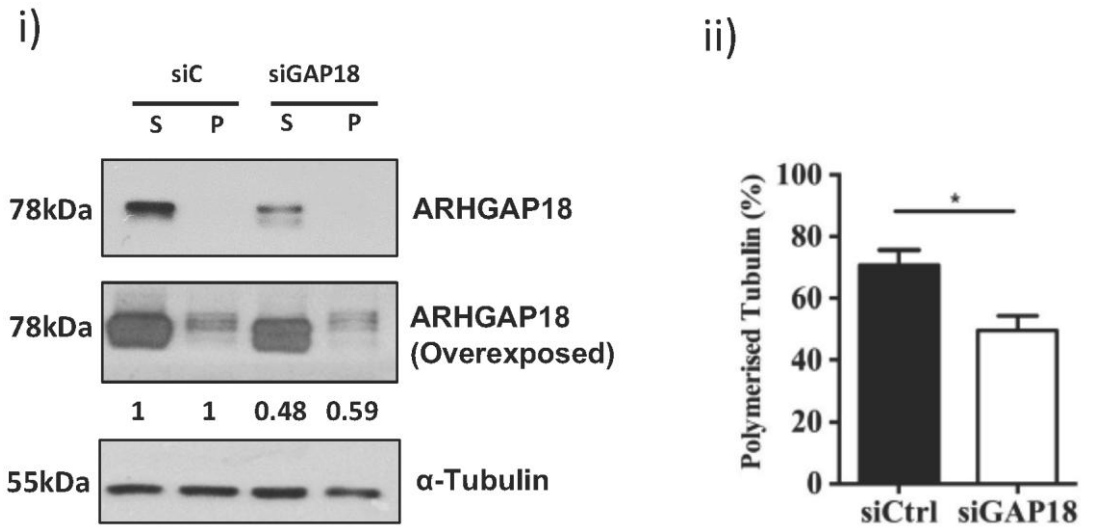

Fig.S6 ARHGAP18 depletion decreases MT stability

ECs were transfected with control siRNA (siC) or siRNA for ARGAP18 (siGAP18), lysed after 48 hours and soluble and polymerised tubulin fractions were separated as given in M&M. ECs were treated with paclitaxel for 4h prior to lysis. Fractions were then analysed by western blotting and probed for ARHGAP18 and α-tubulin.

(i) Representative Western blot and comparative densitometry levels of ARHGAP18 in soluble and polymerised fractions from control or ARHGAP18 KD cells. The levels of ARHGAP18 in the siC cells in both the soluble and polymerised fractions are normalised to 1.0.Representative of five independent experiments. S: soluble tubulin fraction; P:polymerised tubulin fraction.(ii) Percentage of polymerised tubulin. Densitometry readings from 5 independent experiments mean ± SEM, *$p<0.05$.

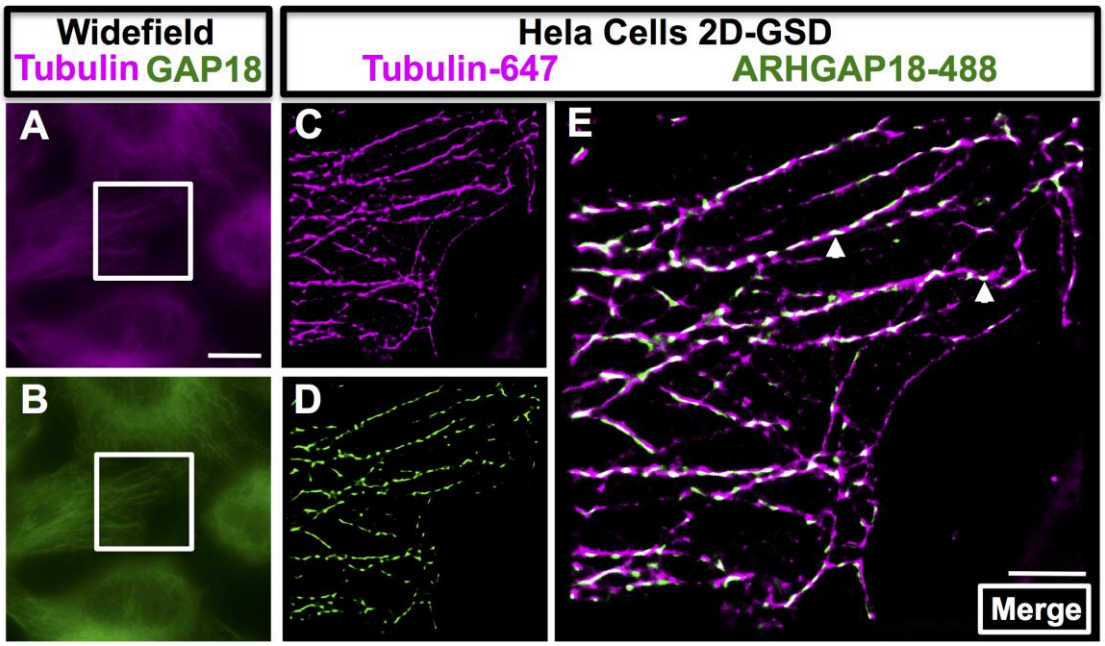

Fig.S7 **ARHGAP18 is localised to microtubules in HeLa cells**. Widefield imaging of HeLa cells stained for ARHGAP18 and α-tubulin, which showed a fibrous-like distribution of ARHGAP18 (**B**), which overlapped with that of α-tubulin (**A**). The white box indicates the area imaged in GSD mode in images (**C**) and (**D**). (**E**) Merged image. Abundant co-localisation is observed of ARHGAP18 puncta along the microtubule filaments as evidenced by the white colour of the merged channel (examples of puncta also shown by white arrowheads). In contrast with ECs, there was much less cytosolic localisation of ARHGAP18 in HeLa cells. Scale bar in **A**= 10μm, **E**= 2.5μm.